JOURNAL OF GEOPHYSICAL RESEARCH, VOL. 102, NO. C4, PAGES 8555–8571, APRIL 15, 1997

Subtidal velocity correlation scales on the northern California shelf

E. P. Dever[1]

Woods Hole Oceanographic Institution, Woods Hole, Massachusetts

Abstract. Along- and cross-shelf correlation scales of subtidal cross-shelf (u) and along-shelf (v) velocities are estimated using moored records from several field programs over the northern California shelf. Over record lengths of 4–6 months, along-shelf correlation scales of v are greater than maximum mooring separations (60 km). In the cross-shelf direction, v is generally correlated between the 60 and 130 m isobaths (10–15 km separation). Along-shelf correlation scales of u are much smaller than those of v and are often not resolved by minimum mooring separations. Time series between November 1988 and May 1989 do resolve along-shelf correlation scales of near-surface u and indicate that they are 15–20 km. During this time the along-shelf correlation scale of near-surface u shows variability on a monthly scale. It is generally long (30 km or more) when correlation of u with wind stress is high and short (15 km or less) when correlation with wind stress is low. On at least one occasion, short along-shelf correlation scales coincide with the intrusion of an offshore mesoscale feature onto the shelf. Cross-shelf correlation scales of u are resolved for typical mooring separations. In general, u is correlated between the 90 and 130 m isobaths (7–13 km separation) and between the 60 and 90 m isobaths (~5 km).

1. Introduction

There exists a considerable body of theory concerning the dynamics of subtidal velocity on wind-driven shelves [*Allen*, 1980]. This includes surface and bottom boundary layer theory [*Brink*, 1983; *Lentz*, 1992; *Trowbridge and Lentz*, 1991], two-dimensional upwelling models [*Csanady*, 1982; *Janowitz and Pietrafesa*, 1980; *Mitchum and Clarke*, 1986], and coastal-trapped waves (CTW) theory [*Chapman*, 1987; *Brink*, 1991]. These theories often assume the circulation is two-dimensional or, at most, slowly varying in the along-shelf direction.

Observational estimates of along-shelf velocity (v) correlation lengths over wind-forced shelves [*Kundu and Allen*, 1976; *Winant et al.*, 1987] generally agree with this theoretical assumption, and subtidal v can be correlated over along-shelf distances greater than maximum mooring separations (60 km and more). The long v correlation scales observed when wind stress forcing dominates do not preclude shorter correlation scales when wind stress forcing is less important [*Winant*, 1983].

Understanding cross-shelf flow remains a major challenge in coastal oceanography [*Smith*, 1995]. However, along-shelf scales of subtidal cross-shelf velocity (u) are not only shorter than those predicted by wind-forced theory but have usually not been resolved [e.g., *Kundu and Allen*, 1976; *Winant et al.*, 1987; *Winant*, 1983]. Successful estimates should therefore provide insight into the dynamics of u and how observed velocities differ from simple wind-forced theory. They may also contribute to a better understanding of the spatial scales over which point measurements apply to u on wind-driven shelves which should be useful to interpretation of existing measurements and to future experiment design.

The objectives of this study are to summarize the spatial scales of both subtidal v and u on the northern California shelf and to gain insight into the processes which affect u spatial scales in particular. The spatial scales will be defined here in terms of correlation lengths, the length over which subtidal fluctuations are correlated at some significance level. They will be estimated from time series lasting several months and encompassing all seasons.

The remainder of the paper is divided into five sections. In section 2 I give a brief overview of the general conditions over the northern California shelf and an introduction to the field programs used. In section 3 I list the procedures used to estimate u and v correlation scales and give results for the various experiments. In section 4 the u correlation scales between November 1988 and May 1989 are further examined with a view to identifying the processes which affect them. In section 5 I compare the observed correlation scales with those expected from wind-forced theory. In section 6 the results are summarized.

2. Background and Observations

2.1. Background

The region examined in this study extends from Point Reyes to Point Arena (Figures 1 and 2). It is noted for its strong along-shelf wind forcing and relatively straight narrow shelf [*Beardsley and Lentz*, 1987], and in these respects it is perhaps an archetype of wind-forced circulation present along much of the U.S. Pacific coast and elsewhere. Wind stress here exhibits strong seasonal variability. In winter and spring it is distinguished by weak monthly means and poleward and equatorward fluctuations on timescales of days. In summer it is distinguished by strong monthly means with periods of upwelling favorable stress which persist for several weeks [*Halliwell and*

[1]Now at Center for Coastal Studies, Scripps Institution of Oceanography, La Jolla, California.

Paper number 96JC03451.
0148-0227/97/96JC-03451$09.00

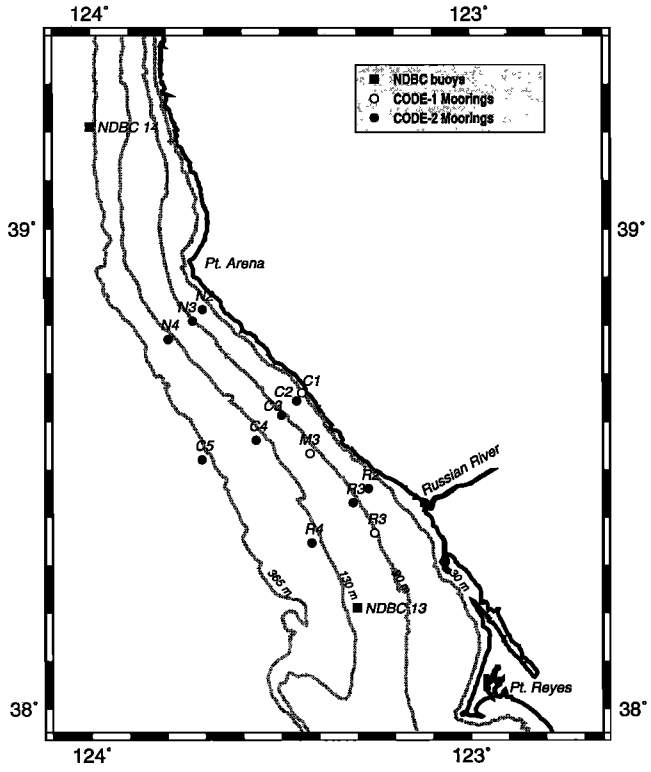

Figure 1. Map of northern California shelf showing nominal Coastal Ocean Dynamics Experiment (CODE) (circles) and National Data Buoy Center (NDBC) (solid squares) mooring locations. Exact locations varied slightly from deployment to deployment, and most locations included nearby surface and subsurface components. Solid circles denote locations occupied during CODE-2, and open circles denote locations occupied during CODE-1. The central C line (with the exception of C1) was present during both CODE-1 and CODE-2. The southerly R3 location was occupied during CODE-1 and fall and winter CODE deployments but was later moved north during CODE-2.

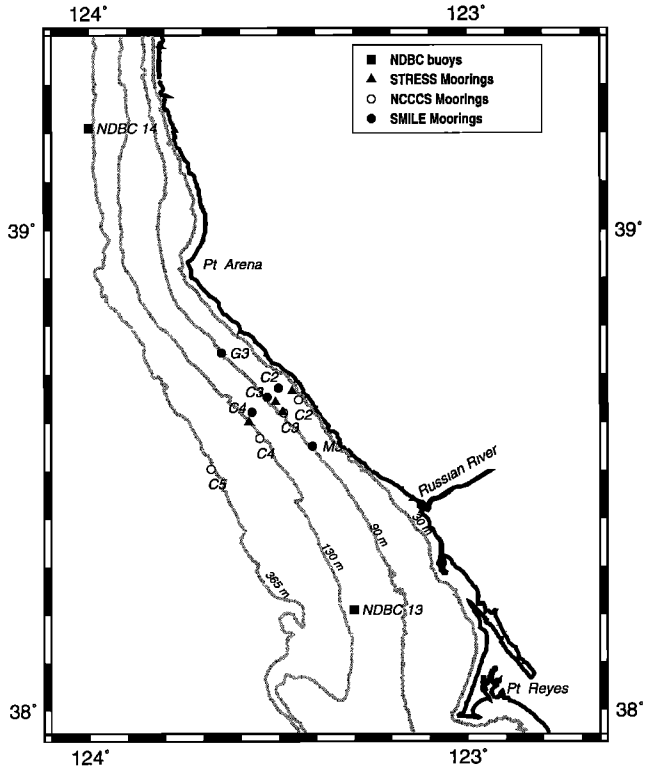

Figure 2. Map of northern California shelf showing nominal Northern California Coastal Circulation Study (NCCCS) (open circles), Shelf Mixed Layer Experiment (SMILE) (solid circles), Sediment Transport Events over the Shelf and Slope (STRESS) (solid triangles), and NDBC (solid squares) mooring locations. NCCCS mooring locations varied slightly from deployment to deployment.

Allen, 1987; *Strub et al.*, 1987; *Beardsley et al.*, 1987]. Figure 3 shows that the low-frequency along-shelf wind stress has long spatial scales in all seasons [see also *Beardsley et al.*, 1987]. Data used to estimate the correlation scales of along-shelf wind stress are shown in Table 1.

2.2. Field Programs

In part because of the characteristics listed above, the northern California shelf has been the site of several large field programs. These include the Coastal Ocean Dynamics Experiment (CODE) [see, e.g., *Beardsley and Lentz*, 1987; *Winant et al.*, 1987; *Lentz and Chapman*, 1989], Northern California Coastal Circulation Study (NCCCS) [*Largier et al.*, 1993], Shelf Mixed Layer Experiment (SMILE) [*Dever and Lentz*, 1994], and Sediment Transport Events over the Shelf and Slope (STRESS) study. Nominal mooring locations used here are shown for CODE in Figure 1 and for SMILE, STRESS, and NCCCS in Figure 2. Table 2 lists the exact locations and start and stop times of time series used in this study. Comprehensive information concerning these moored measurements are given by *Rosenfeld* [1983], *Limeburner* [1985], *EG&G, Inc.* [1989, 1990a, b], *Alessi et al.* [1991], and *Fredericks et al.* [1993].

3. Velocity Correlation Length Scales

3.1. Procedures

Correlations were estimated from low-pass filtered velocity records (Table 2). The PL64 filter used has a 38 hour half-power point and is described by *Limeburner* [1985]. Record

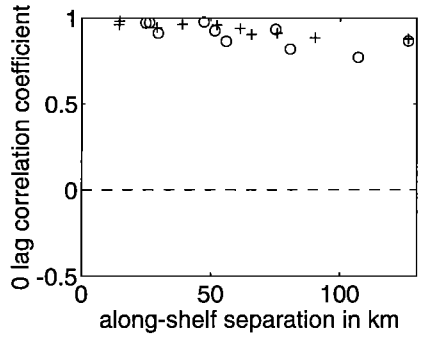

Figure 3. Correlations of low-passed along-shelf wind stress, τ^y, as a function of along-shelf mooring separation for summer (CODE-2) NDBC 14, N3, C3, R3, and NDBC 13 (open circles) and winter and spring (SMILE) NDBC 14, G3, C3, M3, and NDBC 13 (pluses). The along-shelf direction is defined as 317°T for all locations except for the NDBC 14 location where it is defined as 341°T. Correlation scales of τ^y are not sensitive to the precise definition of along-shelf direction and exceed 100 km.

Table 1. Data Used to Estimate Along-Shelf Wind Stress Correlation Scales

Mooring	Position		Principle Axis, °T	$\overline{\tau^x}$, dyn cm^{-2}	$\overline{\tau^y}$, dyn cm^{-2}	σ_x, dyn cm^{-2}	σ_y, dyn cm^{-2}	T_x, hours	T_y, hours
	Latitude	Longitude							
CODE-2: 0400 UT, April 5, 1982, to 2100 UT, July 25, 1982									
NDBC14	39°11.98′	124°00.00′	333	−0.1	−0.9	0.2	1.3	47	44
C3	38°36.40′	123°27.70′	313	0.1	−1.1	0.1	1.3	58	58
R3	38°25.33′	123°16.36′	313	0.1	−1.0	0.1	1.2	53	55
NDBC13	38°11.98′	123°18.00′	312	0.2	−1.0	0.2	1.2	53	57
CODE-2: 0400 UT, April 11, 1982, to 2100 UT, July 25, 1982									
N3	38°48.07′	123°41.71′	335	−0.3	−1.0	0.1	1.1	46	46
SMILE: 0700 UT, Nov. 16, 1988, to 1100 UT, April 6, 1989									
G3	38°44.40′	123°36.40′	342	−0.3	−0.2	0.3	0.8	38	38
SMILE: 0700 UT, Nov. 16, 1988, to 1900 UT, May 13, 1989									
C3	38°38.71′	123°29.56′	311	0.0	−0.4	0.1	0.9	38	38
M3	38°32.67′	123°22.97′	312	−0.0	−0.3	0.1	0.8	38	38
NDBC13	38°11.98′	123°18.00′	303	0.1	−0.4	0.3	0.9	38	43
SMILE: 1200 UT, Jan. 15, 1989, to 0100 UT, May 4, 1989									
NDBC14	39°11.98′	124°00.00′	342	−0.0	−0.0	0.1	0.9	38	38

Start and stop times given are those used for correlation calculations. The along-shelf direction is taken as 317°T except at NDBC 14 where it is taken as 341°T.

start and stop times were chosen such that complete records existed at most moorings in any given field program deployment. To compare NCCCS and SMILE, the NCCCS records were divided into three periods, the second of which coincided with SMILE. Record lengths ranged from 90 to 200 days (Table 2). The (one-sided) autocorrelation timescales provide an estimate of the number of degrees of freedom for cross correlations between two time series. Autocorrelation timescales were generally 3–4 days for v and 2–3 days for u. Longer time series also tend to have longer autocorrelation times as they start to pick up seasonal variability. The autocorrelation timescales generally suggest at least 30 degrees of freedom. This estimate is conservative in that cross-correlation timescales are always less than autocorrelation timescales. For 30 degrees of freedom, correlations of 0.30 (0.35) or greater are significant at the 90% (95%) level.

Velocity records were rotated into local isobath reference frames at each mooring location (Table 2). The CODE-2 local isobath directions [*Winant et al.*, 1987] were also used for the analogous CODE-1, NCCCS, SMILE, and STRESS locations. The CODE-1 C1 isobath orientation is given by *Lentz* [1994], while the CODE-1 R3 and M3 and the SMILE M3 and G3 isobath orientations were estimated from charts. As noted by *Smith* [1981], u is sensitive to the reference frame. To test this, correlations were calculated in which all records were rotated ±2° and ±5° from the local isobaths. The v correlation coefficients varied by only ±0.02. Correlation coefficients for u showed more scatter (about ±0.10). Sensitivity of u correlations to coordinate rotation was greatest for near-bottom instruments and those located at the 30 or 60 m isobath. However, qualitative results were unaffected in that u correlations which were significant in the local isobath reference frame remained significant in the rotated reference frames.

Correlations were calculated for near-surface, middepth, and near-bottom records. These depths were chosen based on the division of flow into a surface boundary layer, an inviscid interior (except at the 30 m C1 site), and a bottom boundary layer. Near-surface records were at 10 m, or failing that, at the shallowest available depth (always 20 m or less). Generally, these records were in the surface boundary layer, though several are probably below it during weak wind stress conditions, especially in summer [*Lentz*, 1992]. Middepth records were as near as possible to half the water depth at each mooring. Near-bottom velocity records were 10 to 20 m above the bottom. Though 20 m is near the upper limit of bottom boundary layer [*Lentz and Trowbridge*, 1991], it was felt the larger number of records gained was preferable to the limited records within 10 m of the bottom.

3.2. Along-Shelf Correlation Scales

Correlations as a function of along-shelf separation were estimated primarily along the 90 m isobath. Additional estimates along the 60 and 130 m isobaths were made using the CODE-2 data. Minimum along-shelf separations ranged from 4 km during the common SMILE/NCCCS time period to 26 km in CODE-2.

Along-shelf velocities (Figure 4 and Table 3) were significantly correlated at all along-shelf mooring separations for near-surface, middepth, and near-bottom depths; hence v along-shelf correlation scales are greater than 60 km in this area. Correlations appear to show little variation between field programs which occurred during different seasons. Though correlated at all depths, correlations of interior and near-bottom v were slightly larger than near-surface v (Table 3 and Figure 4). Along-shelf correlations of v are not a strong function of total water depth though CODE-2 observations suggest some decrease in near-surface v correlation at the 130 m isobath (N4, C4, and R4) relative to the 60 (N2, C2, and R2) and 90 m (N3, C3, and R3) isobaths (Table 3).

Along-shelf correlation scales of u (Figure 5 and Table 3) were resolved only for near-surface u during SMILE and NCCCS (and possibly by CODE-1 C3 and M3) along the 90 m isobath. SMILE and NCCCS correlations indicate that along-shelf correlation scales of near-surface u are from 15 to 20 km. Little information is available about subsurface u along-shelf correlation scales. There is the suggestion that middepth and near-bottom u are correlated at separations of 4–10 km but that correlation lengths are less than 25 km.

Table 2. Velocity Data Used to Estimate Correlation Scales

Mooring	Position		Instrument Depth, m	Water Depth, m	Isobath, °T	$\bar{u}$, 10^{-2} m s^{-1}	$\bar{v}$, 10^{-2} m s^{-1}	σ_u, 10^{-2} m s^{-1}	σ_v, 10^{-2} m s^{-1}	T_u, hours	T_v, hours	Principle Axis, °T
	Latitude	Longitude										
CODE-1: 0400 UT, April 17, 1981, to 1500 UT, July 10, 1981												
C1	38°39.80′	123°25.10′	4	30	335	−1.6	−3.4	1.2	6.1	38	38	344
C1	38°39.80′	123°25.10′	27	30	335	0.4	1.0	1.0	4.1	38	40	344
C2	38°39.20′	123°25.60′	4	63	325	−4.4	−2.4	3.8	12.1	38	54	340
C3	38°36.38′	123°27.71′	9	90	317	−9.8	−12.7	4.5	24.0	38	46	330
C3	38°37.20′	123°28.30′	39	90	317	−2.7	−2.3	4.5	19.5	40	51	342
C3	38°37.20′	123°28.30′	83	90	317	−0.5	0.4	2.7	13.7	42	45	315
C4	38°34.50′	123°32.60′	19	133	319	−6.3	−22.8	9.1	21.2	45	58	330
C4	38°34.50′	123°32.60′	65	133	319	−1.2	−9.1	5.7	14.4	46	56	322
C4	38°34.50′	123°32.60′	123	133	319	−1.1	−1.6	4.5	10.3	39	46	312
C5	38°31.27′	123°40.41′	9	402	330	−6.5	−23.5	14.4	21.1	54	52	16
C5	38°31.27′	123°40.41′	152	402	330	1.9	−0.6	5.0	14.5	53	91	340
M3	38°31.60′	123°23.20′	9	90	317	−4.0	−1.4	4.8	22.9	44	61	331
M3	38°31.60′	123°23.30′	55	90	317	2.7	2.8	4.1	18.5	50	56	330
M3	38°31.60′	123°23.30′	74	90	317	1.3	4.3	3.6	17.2	43	54	317
R3	38°21.60′	123°13.00′	9	90	336	−3.8	−5.6	4.2	15.2	38	66	347
R3	38°21.65′	123°13.00′	55	90	336	2.6	1.3	3.2	12.1	43	58	324
R3	38°21.65′	123°13.00′	75	90	336	2.2	2.5	2.7	10.9	51	51	316
CODEW2: 0400 UT, Aug. 7, 1981, to 2100 UT, Dec. 7, 1981												
C3	38°36.11′	123°27.18′	9	90	317	−1.9	7.6	4.2	18.9	76	121	337
C3	38°36.19′	123°27.18′	55	90	317	4.6	9.4	2.1	13.1	75	87	333
C3	38°36.19′	123°27.18′	75	90	317	0.3	8.1	1.5	11.1	38	76	319
C5	38°31.30′	123°40.10′	150	400	330	0.5	4.4	4.1	9.6	52	88	337
R3	38°21.80′	123°13.00′	9	90	336	−1.4	6.4	5.2	12.8	38	80	356
R3	38°21.70′	123°13.10′	55	90	336	1.3	7.2	2.1	9.0	38	78	332
R3	38°21.70′	123°13.10′	75	90	336	−0.7	5.1	1.7	8.2	38	66	327
CODEW3: 0400 UT, Dec. 16, 1981, to 2100 UT, March 19, 1982												
C3	38°36.11′	123°27.18′	9	90	317	−1.6	3.5	6.3	21.3	42	58	332
C3	38°36.10′	123°27.40′	55	90	317	2.0	5.6	2.9	11.6	38	51	324
C3	38°36.10′	123°27.40′	75	90	317	0.6	5.4	2.4	8.8	38	39	320
C5	38°31.30′	123°40.60′	9	400	330	−0.8	−7.3	8.8	15.2	77	104	12
C5	38°31.30′	123°40.10′	150	400	330	1.7	3.6	5.0	12.2	63	105	337
R3	38°21.50′	123°13.00′	9	90	336	−0.3	0.2	6.5	14.3	38	51	345
R3	38°21.95′	123°13.15′	55	90	336	1.3	3.4	2.4	9.9	38	40	328
R3	38°21.95′	123°13.15′	75	90	336	0.4	3.5	2.3	9.1	38	38	323
CODE-2: 0400 UT, April 5, 1982, to 2100 UT, July 25, 1982												
C2	38°38.16′	123°25.32′	10	60	325	−1.8	3.6	2.5	19.3	38	62	323
C2	38°38.16′	123°25.32′	35	60	325	0.4	3.5	2.7	13.3	90	61	325
C2	38°38.16′	123°25.32′	53	60	325	−0.4	1.9	1.1	8.2	44	60	321
C3	38°38.38′	123°27.71′	10	93	317	−3.8	−6.4	6.6	24.9	53	76	327
C3	38°34.30′	123°32.70′	53	90	317	0.7	0.5	2.7	15.7	65	74	324
C3	38°34.30′	123°32.70′	83	90	317	0.0	0.9	1.8	11.6	38	65	314
C4	38°33.26′	123°31.68′	10	130	319	−7.3	−20.7	9.2	21.9	38	98	332
C4	38°33.26′	123°31.56′	70	130	319	0.7	−4.7	4.6	12.3	38	69	320
C4	38°33.26′	123°31.56′	121	130	319	0.1	1.4	3.4	10.7	38	49	314
C5	38°30.80′	123°40.25′	20	400	330	0.7	−16.9	9.5	19.6	54	160	337
C5	38°30.88′	123°40.41′	150	400	330	1.9	4.8	3.8	11.7	56	133	332
N2	38°49.50′	123°40.11′	10	60	316	−2.1	−2.7	4.0	25.9	46	61	316
N2	38°49.50′	123°40.11′	35	60	316	1.1	1.7	1.7	15.7	43	60	308
N3	38°48.07′	123°41.71′	10	90	319	−3.8	−8.3	6.0	28.9	73	60	325
N3	38°48.09′	123°41.77′	53	90	319	1.9	2.1	2.6	17.1	43	60	315
N3	38°48.09′	123°41.77′	83	90	319	−0.8	3.5	3.3	13.9	55	53	302
N4	38°45.79′	123°45.60′	10	129	319	−5.6	−17.3	9.0	24.4	81	110	338
N4	38°45.71′	123°45.55′	70	130	319	1.6	−2.3	4.6	15.0	92	80	322
N4	38°45.71′	123°45.55′	121	130	319	1.0	4.3	3.3	14.0	49	55	305
R2	38°27.17′	123°13.97′	20	60	319	1.4	6.5	3.0	13.7	42	49	316
R2	38°27.14′	123°13.94′	35	60	319	1.4	5.8	1.9	10.6	38	50	310
R2	38°27.14′	123°13.94′	53	60	319	0.2	3.1	1.7	6.3	38	50	310
R3	38°25.38′	123°16.40′	20	90	329	0.2	−0.0	4.1	17.8	45	61	333
R3	38°25.33′	123°16.36′	53	90	329	0.6	1.2	2.3	12.4	48	59	323
R3	38°25.38′	123°16.40′	70	90	329	0.5	1.6	1.9	11.9	50	57	317
R4	38°20.36′	123°22.94′	10	130	339	−0.7	−18.3	6.8	18.4	40	85	347
R4	38°20.84′	123°22.95′	70	130	339	1.8	−4.9	5.2	9.9	38	70	333
R4	38°20.84′	123°22.95′	110	130	339	−0.1	−0.1	4.0	7.9	45	59	322
NCCCS: 0100 UT, March 23, 1988, to 0000 UT, Aug. 16, 1988												
C2	38°38.33′	123°24.60′	10	60	325	−0.0	−1.3	2.1	17.5	101	103	317

Table 2. (continued)

Mooring	Position		Instrument Depth, m	Water Depth, m	Isobath, °T	$\bar{u}$, 10^{-2} m s^{-1}	$\bar{v}$, 10^{-2} m s^{-1}	σ_u, 10^{-2} m s^{-1}	σ_v, 10^{-2} m s^{-1}	T_u, hours	T_v, hours	Principle Axis, °T
	Latitude	Longitude										
NCCCS: 0100 UT, March 23, 1988, to 0600 UT, Nov. 16, 1988												
C3	38°36.77′	123°26.93′	10	90	317	−3.0	−6.1	5.5	23.4	65	434	321
C3	38°36.77′	123°27.48′	45	90	317	2.1	2.7	2.7	14.4	156	194	324
C3	38°36.77′	123°26.93′	75	90	317	1.3	3.4	3.1	7.2	55	76	300
C4	38°33.60′	123°30.78′	10	130	319	−8.0	−17.9	7.1	21.5	215	268	348
C5	38°30.00′	123°38.55′	150	400	330	0.8	7.0	3.3	6.6	92	102	330
NCCCS: 0900 UT, May 4, 1988, to 0700 UT, Aug. 17, 1988												
C5	38°30.35′	123°39.73′	10	400	330	−1.3	−19.6	13.0	22.0	105	101	360
NCCCS: 0700 UT, Nov. 16, 1988, to 0100 UT, Feb. 12, 1989												
C5	38°30.00′	123°38.55′	150	400	330	−1.2	6.9	3.3	8.8	47	92	318
NCCCS: 0700 UT, Nov. 16, 1988, to 1900 UT, May 13, 1989												
C3	38°36.77′	123°26.93′	10	90	317	−1.5	−3.9	5.2	17.4	47	108	325
C3	38°36.77′	123°27.48′	45	90	317	2.8	3.7	2.7	11.4	85	92	319
C3	38°36.77′	123°26.93′	75	90	317	0.2	3.7	2.3	8.1	55	56	310
C4	38°33.60′	123°30.78′	10	130	319	−3.2	−13.5	7.3	17.5	110	162	329
NCCCS: 0200 UT, Feb. 21, 1989, to 1900 UT, May 13, 1989												
C2	38°38.33′	123°24.60′	10	60	325	−1.9	−2.9	2.1	17.1	47	62	339
NCCCS: 2000 UT, May 13, 1989, to 2300 UT, Oct. 17, 1989*												
C2	38°38.33′	123°24.60′	10	60	325	1.2	4.6	2.0	13.2	68	75	339
C3	38°36.77′	123°26.93′	10	90	317	−4.3	−6.8	4.4	27.0	66	103	323
C3	38°36.77′	123°27.48′	45	90	317	0.6	−5.2	3.1	19.3	38	60	320
C3	38°36.77′	123°26.93′	75	90	317	1.0	4.1	2.8	11.5	54	72	307
C4	38°33.60′	123°30.78′	10	130	319	−5.6	−19.1	6.4	21.6	49	213	327
SMILE: 0700 UT, Nov. 16, 1988, to 1400 UT, April 21, 1989												
C3	38°38.71′	123°29.56′	11.5	93	317	−2.2	−3.3	4.3	14.4	38	104	325
SMILE: 0700 UT, Nov. 16, 1988, to 1900 UT, May 13, 1989												
C3	38°38.71′	123°29.56′	44.5	93	317	1.7	1.8	2.3	10.9	52	92	320
C4	38°36.78′	123°31.87′	10	117	319	−5.5	−12.0	7 8	17.3	95	149	337
C4	38°36.78′	123°31.87′	52	117	319	0.4	−4.1	3.8	13.3	109	134	327
G3	38°44.40′	123°36.40′	10	93	317	−3.6	−5.9	5.7	16.1	95	118	322
M3	38°32.67′	123°22.97′	10	93	317	−4.2	−4.0	4.6	17.4	38	115	326
SMILE: 0400 UT, Feb. 28, 1989, to 1900 UT, May 13, 1989												
C2	38°39.80′	123°27.82′	10	80	325	−2.6	−8.5	4.9	18.8	38	59	326
STRESS-1: 1800 UT, Dec. 8, 1988, to 0700 UT, Feb. 25, 1989												
C3	38°38.44′	123°29.64′	79	97	317	−0.1	5.7	1.8	7.6	38	43	313
C3	38°38.44′	123°29.64′	91	97	317	−1.3	3.5	1.9	6.8	38	38	309
STRESS-1: 1200 UT, March 6, 1989, to 0100 UT, May 5, 1989												
C3	38°38.14′	123°29.97′	77	95	317	−0.3	1.5	1.9	9.9	38	50	314
STRESS-1: 1000 UT, Dec. 9, 1988, to 0300 UT, Feb. 24, 1989												
C3′	38°36.89′	123°27.18′	86	92	317	−0.6	4.2	1.9	6.7	38	38	313
STRESS-2: 1900 UT, Nov. 23, 1990, to 0600 UT, March 7, 1991												
C2	38°39.50′	123°25.64′	39	49	325	0.7	4.8	1.4	7.1	38	47	323
C3	38°38.14′	123°28.31′	59	90	317	1.9	9.8	2.7	12.1	38	64	317
C3	38°38.14′	123°28.31′	80	90	317	−1.0	5.9	1.9	8.9	38	51	310
C4	38°35.64′	123°32.52′	59	130	319	1.3	3.1	4.0	15.8	46	105	328
C4	38°35.64′	123°32.52′	120	130	319	−0.3	3.8	2.4	9.6	38	49	312

Start and stop times given are those used for correlation calculations.
*From overlapping multiple deployments, position given is recorded position in Scripps Data Zoo files (deployment 1).

3.3. Cross-Shelf Correlation Scales

Correlations as a function of cross-shelf separation were estimated primarily along the C line. Moorings along the C line ranged from the inner shelf to the outer shelf, and separations were from 1 to 12 km becoming progressively larger offshore. Additional estimates of cross-shelf correlations were made along the CODE-2 N and R lines.

Cross-shelf scales in general are more difficult to interpret than along-shelf correlation scales. For a straight shelf with large-scale wind forcing, interpretation of along-shelf correlation scales is fairly straightforward in that we expect along-shelf correlations to be primarily a function of separation and not along-shelf position. In contrast, there is no reason to expect cross-shelf correlation scales to be independent of cross-shelf position. Coastal oceanographers often divide shelves into three regions [see, e.g., *Lentz*, 1995; *Allen et al.*, 1983]: an inner shelf where surface and bottom boundary layers interact, a midshelf where surface and bottom boundary

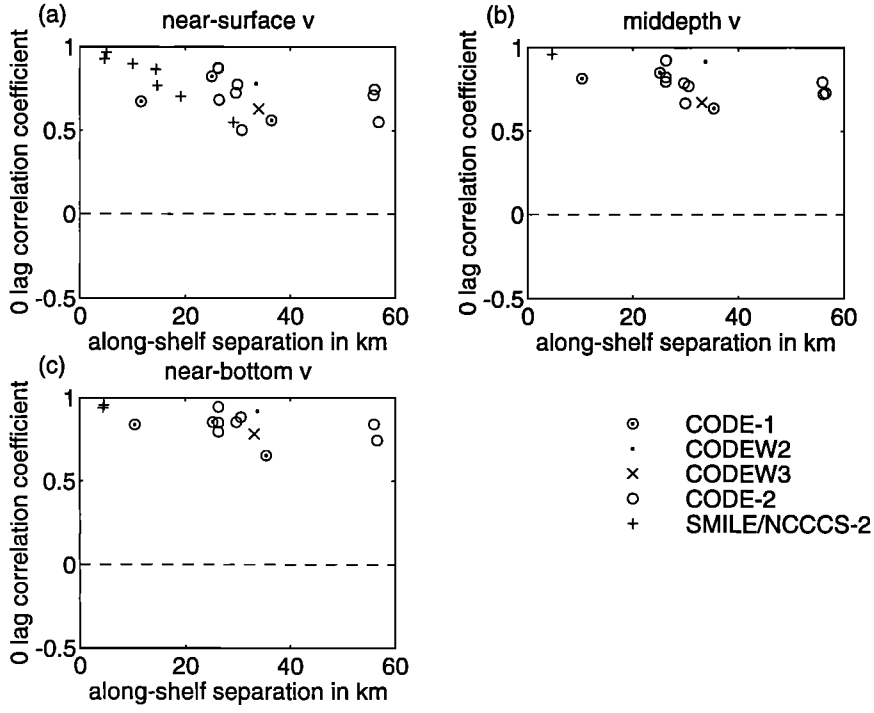

Figure 4. Correlations of along-shelf velocity v as a function of along-shelf mooring separation for (a) near-surface, (b) middepth, and (c) near-bottom instruments. Lags at maximum correlation are usually very close to those at 0 lag, and for consistency, 0 lagged correlations are plotted throughout. Correlations are also presented in Table 3. Along-shelf correlation scales of v exceed the maximum mooring separation (~60 km).

layers are thin compared to the total water depth but where the shelf is generally isolated from off-shelf variability, and an outer shelf where open ocean variability is important. Because the processes which govern the velocity field on the shelf are themselves often a strong function of cross-shelf position, cross-shelf correlations estimated here will be discussed in light of cross-shelf position as well as separation.

Cross-shelf correlation scales of v (Figure 6 and Table 4) are 10–15 km. Despite showing more scatter than v along-shelf correlations, they are well resolved in the sense that observations are significantly correlated to their nearest neighbors. Scatter between experiments again shows no seasonal variability. Most observations are over the 60, 90, and 130 m isobaths. Within this region, v correlations are not a strong function of position; that is, correlations between v at 60 and 90 m (a distance of about 5 km) appear to be about the same as correlations between v at 90 and 130 m (a distance of about 8 km). Similarly, cross-shelf correlations of v exhibit little systematic variability with instrument depth.

Like the along-shelf u correlations, the cross-shelf u correlations were best resolved in the near-surface observations where the cross-shelf correlation scale is about 10 km. In contrast to along-shelf correlations of u, cross-shelf correlations of u (Figure 7 and Table 4) were resolved by typical mooring separations. Comparison of u correlations between the 60 and 90 isobaths with those between 90 and 130 m (mostly from summer observations) gives some suggestion that near-surface u is more highly correlated between the outer-shelf pair despite the greater mooring separation. Though the CODE-2 observations give some indication that u correlations are higher for near-surface and near-bottom instruments than for interior instruments, the large scatter and limited number of time series make definitive statements about depth dependence impossible.

4. Interpreting u Along-Shelf Correlation Length Scales During the Winter and Spring 1988–1989

Both along-shelf and cross-shelf correlation scales of v and cross-shelf correlation scales of u were resolved adequately by most field programs examined in section 3. However, along-shelf u correlations were not resolved by typical along-shelf mooring separations of 30 km, and short mooring separations (5–15 km) are required. This is much shorter than the scale of the along-shelf wind stress (see Figure 3) which is generally acknowledged to be a dominant driving force of near-surface cross-shelf circulation [e.g., *Dever*, 1995; *Lentz*, 1992] and warrants a closer examination.

To gain insight into the processes which reduce along-shelf correlation scales of u, observations from the combined SMILE, STRESS, and NCCCS moorings (Figure 2) are examined here in further detail. These moorings come closest to meeting the requirements for resolving along-shelf scales of u, though spatial coverage is only extensive near the surface. They provide correlation scale estimates for near-surface u from 4 to 30 km along the 90 m isobath between November 1988 and May 1989.

Time series of low-pass filtered along-shelf wind stress (τ^y) and u (Figure 8) show visually that numerous wind forcing events (e.g., December 6–7, December 22–24, March 1, and April 10) are reflected to some extent at all mooring sites. However, there is additional u variability which is not evident

Table 3. Correlations of u and v as a Function of Along-Shelf Separation

Moorings	Hours	Distance, km	0 Lag u Correlations	Max Lag u Correlations	Max Lag Hours	0 Lag v Correlations	Max Lag v Correlations	Max Lag Hours
				Near-Surface Correlations				
CODE-1								
C3(009):M3(009)	2028	11.61	0.47	0.52	−11	0.67	0.73	−13
M3(009):R3(009)	2028	25.00	0.34	0.34	−2	0.82	0.85	−10
C3(009):R3(009)	2028	36.45	0.22	0.23	−5	0.56	0.62	−14
CODEW2								
C3(009):R3(009)	2946	33.56	0.52	0.52	−4	0.78	0.83	−14
CODEW3								
C3(009):R3(009)	2250	34.00	0.28	0.28	−2	0.63	0.64	−6
CODE-2								
C2(010):R2(020)	2682	26.18	0.03	−0.17	−89	0.87	0.87	+1
N2(010):C2(010)	2682	29.98	0.24	0.26	+100	0.78	0.78	−5
N2(010):R2(020)	2682	56.07	0.06	0.13	+100	0.75	0.75	+0
C3(010):R3(020)	2682	26.29	0.03	−0.08	−43	0.87	0.87	−3
N3(010):C3(010)	2682	29.64	0.07	−0.15	−100	0.72	0.74	−9
N3(010):R3(020)	2682	55.89	−0.01	0.19	+49	0.71	0.72	−5
C4(010):R4(010)	2682	26.42	−0.03	0.26	+56	0.68	0.68	−14
N4(010):C4(010)	2682	30.76	0.08	0.21	+55	0.50	0.50	+0
N4(010):R4(010)	2682	56.83	−0.03	−0.20	+49	0.55	0.57	−16
SMILE								
C3(010):NC(010)	3752	4.67	0.73	0.73	+0	0.93	0.93	+0
NC(010):M3(010)	4285	10.04	0.54	0.54	+2	0.90	0.90	+0
G3(010):C3(010)	3752	14.46	0.35	0.37	−4	0.86	0.86	−2
C3(010):M3(010)	3752	14.71	0.48	0.48	+0	0.77	0.77	−2
G3(010):NC(010)	4285	19.12	0.39	0.39	−2	0.70	0.71	−4
G3(010):M3(010)	4285	29.16	0.11	−0.27	−53	0.55	0.55	−4
C4(010):NC(010)	4285	5.02	0.89	0.89	−1	0.97	0.97	+0
				Middepth Correlations				
CODE-1								
C3(039):M3(055)	2028	10.42	0.66	0.67	−2	0.81	0.85	−9
M3(055):R3(055)	2028	25.15	−0.12	−0.28	−43	0.85	0.86	−4
C3(039):R3(055)	2028	35.36	−0.23	−0.30	−17	0.64	0.67	−9
CODEW2								
C3(055):R3(055)	2946	33.74	−0.06	−0.20	−22	0.92	0.93	−6
CODEW3								
C3(055):R3(055)	2250	33.12	−0.06	−0.22	−19	0.67	0.68	−3
CODE-2								
C2(035):R2(035)	2682	26.25	0.22	0.24	+15	0.79	0.80	+4
N2(035):C2(035)	2682	29.98	0 28	0.29	−9	0.67	0.69	−10
N2(035):R2(035)	2682	56.14	0.64	0.64	−1	0.72	0.72	−1
C3(053):R3(053)	2682	26.29	−0.12	−0.12	+7	0.92	0.92	+0
N3(053):C3(053)	2682	29.72	−0.35	−0.37	+14	0.79	0.80	−6
N3(053):R3(053)	2682	55.97	0.28	0.34	−16	0.79	0.80	−3
C4(070):R4(070)	2682	26.28	0.01	0.30	+52	0.82	0.82	+1
N4(070):C4(070)	2682	30.60	−0.08	−0.28	+88	0.77	0.77	−3
N4(070):R4(070)	2682	56 54	0.03	0.23	−57	0.73	0.73	−3
SMILE								
C3(045):NC(045)	4285	4.67	0.56	0.56	+0	0.96	0.96	+0
				Near-Bottom Correlations				
CODE-1								
C3(083):M3(074)	2028	10.42	0.35	0.45	−14	0.84	0.86	−6
M3(074):R3(075)	2028	25.15	0.25	0.36	+17	0.85	0.86	−5
C3(083):R3(075)	2028	35.36	0.44	0.49	+10	0.65	0.68	−8
CODEW2								
C3(075):R3(075)	2946	33.74	0.16	−0.31	−40	0.92	0.93	−5
CODEW3								
C3(075):R3(075)	2250	33.12	0.10	0.26	+15	0.78	0.78	+0
CODE-2								
C2(053):R2(053)	2682	26.25	0.41	0.41	−2	0.80	0.80	+2
C3(083):R3(070)	2682	26.29	0.44	0.44	−1	0.95	0.95	+1
N3(083):C3(083)	2682	29.72	0.31	0.32	−6	0.86	0.86	−3
N3(083):R3(070)	2682	55.97	0.73	0.75	−8	0.84	0.84	−1
C4(121):R4(110)	2682	26.28	0.03	0.16	+56	0.85	0.85	−2
N4(121):C4(121)	2682	30.60	0.34	0.38	−14	0.88	0.88	+0
N4(121):R4(110)	2682	56.54	0.26	0.39	−24	0.75	0.75	−3
SMILE								
C3(079):NC(075)	3268	4.38	0.51	0.51	+2	0.94	0.94	+1
C3(091):C3′(086)	1842	4.58	0.66	0.66	−2	0.96	0.96	−1

Positive lags denote the first listed series leading the second.

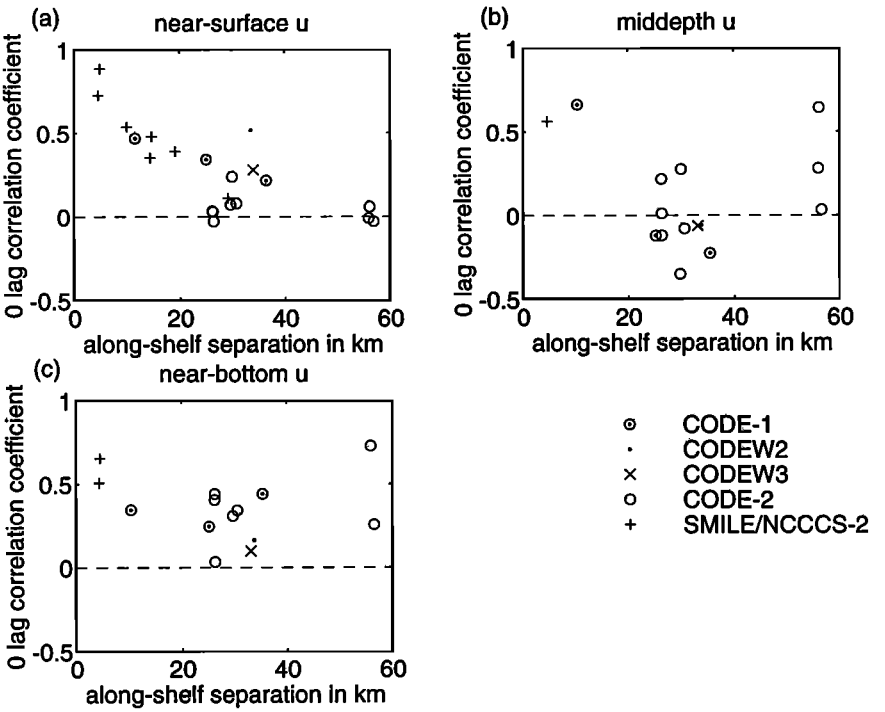

Figure 5. Correlations of cross-shelf velocity u as a function of along-shelf mooring separation for (a) near-surface, (b) middepth, and (c) near-bottom instruments. Correlations are also presented in Table 3. Along-shelf correlation scales of near-surface u are 15–20 km. Along-shelf scales of subsurface u are not well resolved but are less than 25 km.

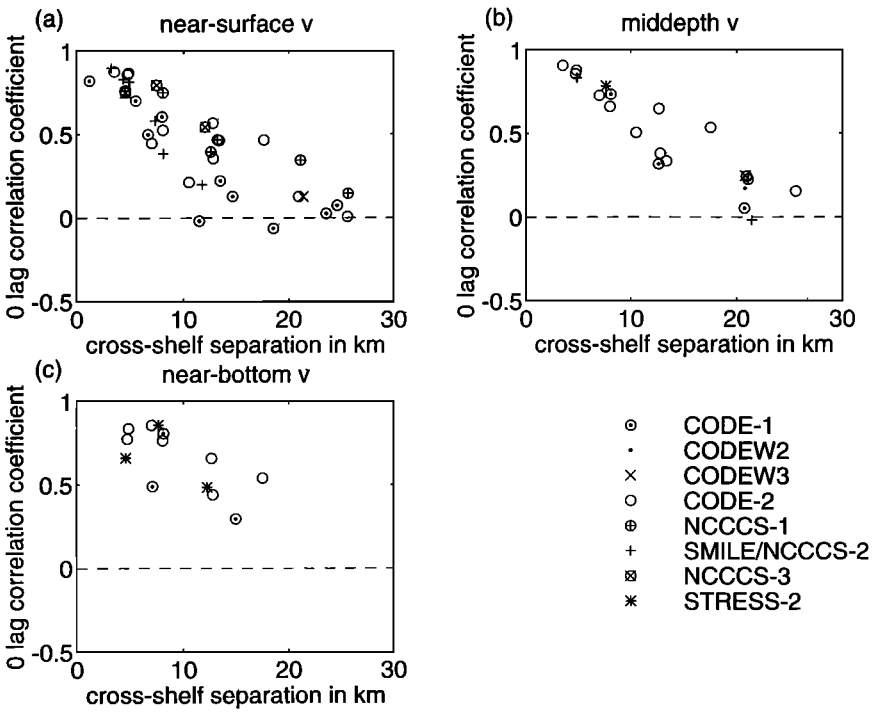

Figure 6. Correlations of along-shelf velocity v as a function of cross-shelf mooring separation for (a) near-surface, (b) middepth, and (c) near-bottom instruments. Correlations are also presented in Table 4. Cross-shelf correlation scales of v are 10–15 km.

Table 4. Correlations of u and v as a Function of Cross-Shelf Separation

Moorings	Hours	Distance, km	0 Lag u Correlations	Maximum Lag u Correlations	Maximum Lag Hours	0 Lag v Correlations	Maximum Lag v Correlations	Maximum Lag Hours
				Near-Surface Correlations				
CODE-1								
C1(004):C2(004)	2028	1.18	0.73	0.73	+1	0.82	0.86	+8
C2(004):C3(009)	2028	5.52	0.42	0.50	+10	0.70	0.79	+13
C1(004):C3(009)	2028	6.68	0.36	0.46	+12	0.50	0.71	+22
C3(009):C4(019)	2028	7.99	0.38	0.39	+8	0.61	0.68	+20
C4(019):C5(009)	2028	11.46	0.15	−0.42	−76	−0.02	0.36	+100
C2(004):C4(019)	2028	13.49	−0.08	−0.21	−29	0.22	0.39	+44
C1(004):C4(019)	2028	14.64	0.09	0.17	+35	0.13	0.41	+53
C3(009):C5(009)	2028	18.53	−0.03	−0.21	−38	−0.06	0.15	+94
C2(004):C5(009)	2028	23.56	0.13	0.17	−74	0.02	−0.14	+43
C1(004):C5(009)	2028	24.60	0.33	0.33	+3	0.07	0.14	−81
CODEW3								
C3(009):C5(009)	2250	21.39	0.49	0.49	−3	0.13	0.22	+89
CODE-2								
N2(010):N3(010)	2682	3.52	0.57	0.57	+2	0.88	0.89	+6
C2(010):C3(010)	2682	4.74	0.30	0.30	+2	0.86	0.87	+8
R2(020):R3(020)	2682	4.86	0.51	0.51	−2	0.87	0.87	+4
N3(010):N4(010)	2682	7.03	0.75	0.75	+2	0.45	0.54	+30
C3(010):C4(010)	2682	8.06	0.66	0.66	+2	0.53	0.58	+23
R3(020):R4(010)	2682	12.77	0.02	0.17	+100	0.57	0.57	+4
N2(010):N4(010)	2682	10.50	0.31	0.35	+12	0.21	0.32	+33
C2(010):C4(010)	2682	12.80	0.04	0.14	+86	0.36	0.42	+24
C4(010):C5(020)	2682	13.37	0.11	−0.23	−78	0.46	0.53	+94
C3(010):C5(020)	2682	20.94	0.00	0.18	+95	0.13	0.18	+68
C2(010):C5(020)	2682	25.57	0.07	0.23	+83	0.01	−0.21	−99
R2(020):R4(010)	2682	17.63	−0.20	−0.20	+3	0.47	0.47	+5
NCCCS-1								
C2(010):C3(010)	3504	4.52	0.38	0.39	−4	0.76	0.77	+8
C3(010):C4(010)	5718	8.06	0.55	0.55	+0	0.75	0.76	+9
C2(010):C4(010)	3504	12.57	0.05	0.11	−53	0.40	0.46	+60
C4(010):C5(010)	2519	13.21	0.44	0.45	+6	0.47	0.57	+100
C3(010):C5(010)	2519	21.11	0.48	0.49	+5	0.34	0.36	−100
C2(010):C5(010)	2488	25.63	0.35	0.35	−3	0.14	0.21	−100
NCCCS-2								
C2(010):C3(010)	1962	4.36	0.44	0.48	−6	0.83	0.83	+2
C3(010):C4(010)	4285	7.37	0.69	0.69	−1	0.58	0.58	+3
C2(010):C4(010)	1962	11.73	0.00	−0.30	+34	0.20	0.21	+9
NCCCS-3								
C2(010):C3(010)	3772	4.57	0.47	0.48	−5	0.75	0.76	+8
C3(010):C4(010)	3772	7.47	0.64	0.65	−1	0.80	0.81	+12
C2(010):C4(010)	3772	12.03	0.24	0.29	−16	0.54	0.57	+27
SMILE								
C2(010):C3(010)	1259	3.23	0.81	0.81	+0	0.90	0.90	+0
C3(010):C4(010)	3752	4.90	0.85	0.85	+1	0.82	0.82	+3
C2(010):C4(010)	1792	8.11	0.75	0.75	+0	0.39	0.39	+6
				Middepth Correlations				
CODE-1								
C3(039):C4(065)	2028	8.13	0.02	−0.30	−72	0.74	0.76	+8
C4(065):C5(152)	2028	12.64	0.06	−0.41	−56	0.32	0.45	+86
C3(039):C5(152)	2028	20.75	−0.36	−0.40	+31	0.05	0.27	−100
CODEW2								
C3(055):C5(150)	2946	20.80	0.13	0.14	−78	0.17	0.17	−3
CODEW3								
C3(055):C5(150)	2250	20.83	0.03	0.16	+75	0.25	0.25	+3
CODE-2								
N2(035):N3(053)	2682	3.55	0.63	0.63	+0	0.91	0.92	+5
C2(035):C3(053)	2682	4.74	0.02	−0.04	−62	0.86	0.87	+6
R2(035):R3(053)	2682	4.86	0.67	0.68	−3	0.88	0.88	+3
N3(053):N4(070)	2682	7.02	0.65	0.65	+1	0.73	0.74	+6
C3(053):C4(070)	2682	8.06	0.29	−0.29	−60	0.66	0.67	+7
R3(053):R4(070)	2682	12.68	0.37	0.44	−13	0.65	0.65	+2
N2(035):N4(070)	2682	10.54	0.41	0.41	+0	0.51	0.53	+10
C2(035):C4(070)	2682	12.80	0.11	0.14	−22	0.38	0.44	+84
C4(070):C5(150)	2682	13.37	0.06	−0.24	−97	0.33	0.34	−8
C3(053):C5(150)	2682	20.94	−0.19	−0.22	−14	0.24	0.24	+1
C2(035):C5(150)	2682	25.57	0.03	−0.12	+100	0.15	0.27	+94
R2(035):R4(070)	2682	17.54	0.23	0.24	−4	0.54	0.54	+4
NCCCS-1								
C3(045):C5(150)	5718	21.11	−0.25	−0.38	−36	0.23	0.24	+100

Table 4. (continued)

Moorings	Hours	Distance, km	0 Lag u Correlations	Maximum Lag u Correlations	Maximum Lag Hours	0 Lag v Correlations	Maximum Lag v Correlations	Maximum Lag Hours
			Middepth Correlations (continued)					
NCCCS-2								
C3(045):C5(150)	2107	21.44	0.19	0.19	+2	−0.02	−0.14	+26
SMILE								
C3(045):C4(052)	4285	4.90	0.50	0.52	−4	0.83	0.83	+0
STRESS-2								
C3(059):C4(059)	2484	7.66	0.47	0.48	+3	0.78	0.78	+0
			Near-Bottom Correlations					
CODE-1								
C1(027):C3(083)	2028	7.12	0.14	0.23	−12	0.49	0.66	+19
C3(083):C4(123)	2028	8.13	0.67	0.68	+3	0.81	0.81	+1
C1(027):C4(123)	2028	15.00	0.17	0.18	−6	0.30	0.44	+18
CODE-2								
C2(053):C3(083)	2682	4.74	0.36	0.37	−3	0.77	0.79	+6
R2(053):R3(070)	2682	4.86	0.70	0.70	+1	0.84	0.85	+6
N3(083):N4(121)	2682	7.02	0.76	0.76	+1	0.85	0.86	+1
C3(083):C4(121)	2682	8.06	0.70	0.70	−1	0.76	0.76	+2
R3(070):R4(110)	2682	12.68	0.50	0.53	−7	0.66	0.66	−3
C2(053):C4(121)	2682	12.80	0.35	0.35	−4	0.44	0.46	+9
R2(053):R4(110)	2682	17.54	0.31	0.34	−7	0.54	0.54	+3
STRESS-2								
C2(039):C3(080)	2484	4.61	0.47	0.47	+2	0.66	0.66	+3
C3(080):C4(120)	2484	7.66	0.58	0.58	+0	0.86	0.86	−1
C2(039):C4(120)	2484	12.26	0.38	0.38	−1	0.48	0.48	+0

Positive lags denote the first listed series leading the second.

everywhere. For example, from early to mid-February offshore flow at 10 m is observed at C3, NCCCS C3, and M3 but is absent at G3. Similarly, in late April, offshore flow is observed at M3, while onshore flow is observed at G3. To better understand the processes which reduce correlation lengths of near-surface u, 28 day subsets of the 6 month time period are next considered. Twenty-eight days was chosen in order to give approximately 10 degrees of freedom per subset. Correlations

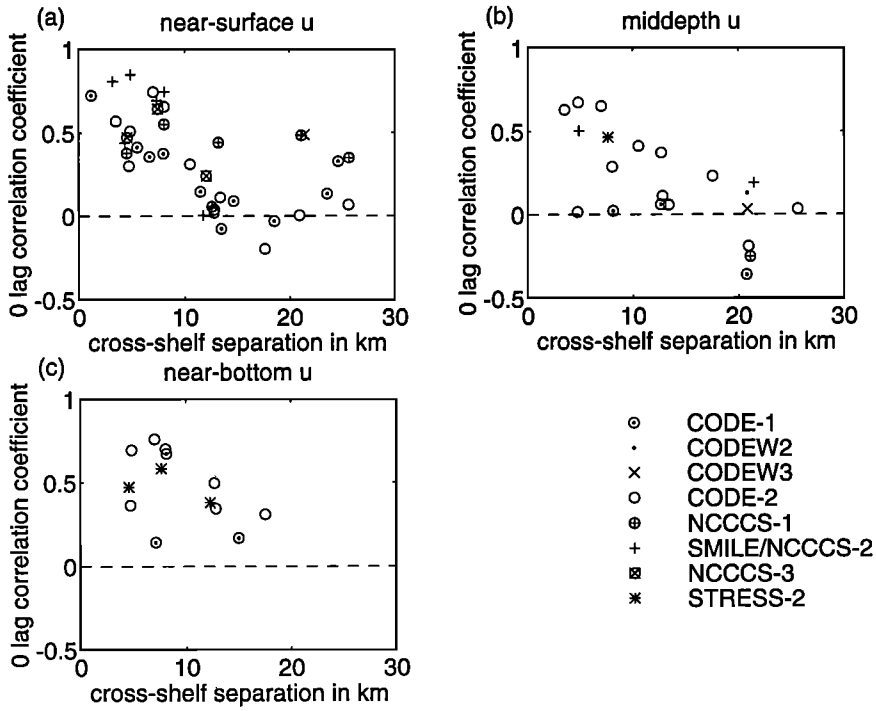

Figure 7. Correlations of cross-shelf velocity u as a function of cross-shelf mooring separation for (a) near-surface, (b) middepth, and (c) near-bottom instruments. Correlations are also presented in Table 4. Cross-shelf correlation scales of u are approximately 10 km.

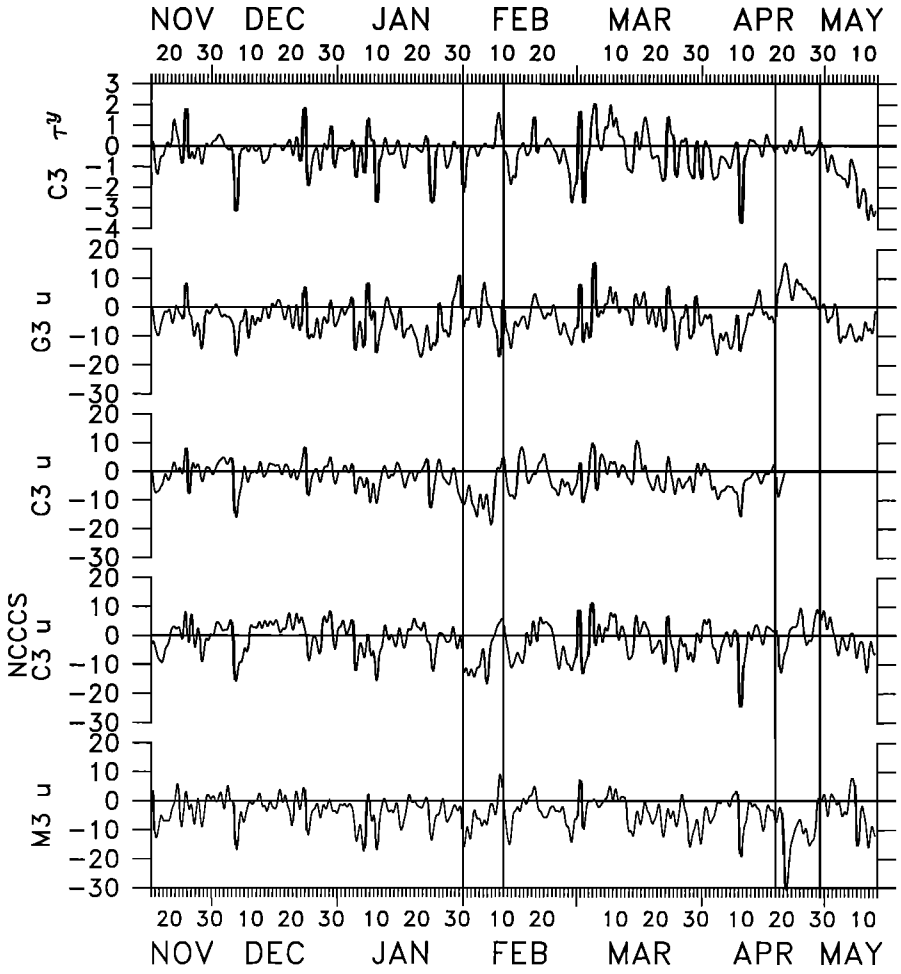

Figure 8. Time series of low-pass filtered τ^y (dyn cm^{-2}) and u (cm s^{-1}) at 10 m. Mooring locations are as denoted in Figure 2. Correlations of u with τ^y range from 0.5 to 0.6. Periods of strong along-shelf variability in early February and late April are bracketed by solid lines.

of 0.50 (0.58) are significant at the 90% (95%) level for 10 degrees of freedom.

4.1. Monthly Variation in Correlation Scales of Near-Surface Cross-Shelf Velocity

Monthly plots of near-surface u correlation as a function of along-shelf separation (Figure 9) show a great deal of variability. From mid-November to mid-January, and again from mid-February to early April, along-shelf correlations show little drop-off as a function of separation. However, from mid-January to early February and again from early April to early May, shorter along-shelf correlation scales exist. Correlation scales are always ≥4 km as the SMILE C3 and NCCCS C3 moorings remain well correlated over all months.

Monthly variability in along-shelf correlation scales of near-surface u appears to be related to the importance of along-shelf wind stress forcing relative to other processes. During months in which correlation length scales are long, all moorings tend to be highly correlated with local wind stress (Table 5). Conversely, when correlation length scales are short, some or most moorings are less well correlated with along-shelf wind stress. Wind stress variability, as indicated by its standard deviation, remains similar through most of the experiment. Therefore lower correlations of near-surface u with along-shelf wind stress are primarily attributed not to a weakening of wind stress but to the greater importance of other processes. However, there is a slight weakening of wind stress variability from mid-January through early February, and this plays a role in reducing correlation with wind stress and hence along-shelf correlation scales.

Between mid-January and early February, near-surface u is well correlated between moorings NCCCS C3 and SMILE C3 and M3 but not between G3 and the other moorings. This suggests a break in cross-shelf circulation between the northern and southern parts of the study area rather than a general increase in short-scale u fluctuations. This along-shelf variability is also marked by a three-dimensional heat balance between January 30 and February 12 [*Dever and Lentz*, 1994, Figure 9] and by a strongly three-dimensional mass balance as indicated by depth-averaged cross-shelf flow at C3 between January 30 and February 20 [*Dever*, 1995]. This depth-averaged cross-shelf flow, which is uncorrelated with the wind, also probably reduces along-shelf correlations of near-surface u between early February and early March (Figure 9) as shifting the start and stop times of the 28 day periods shows reduced along-shelf

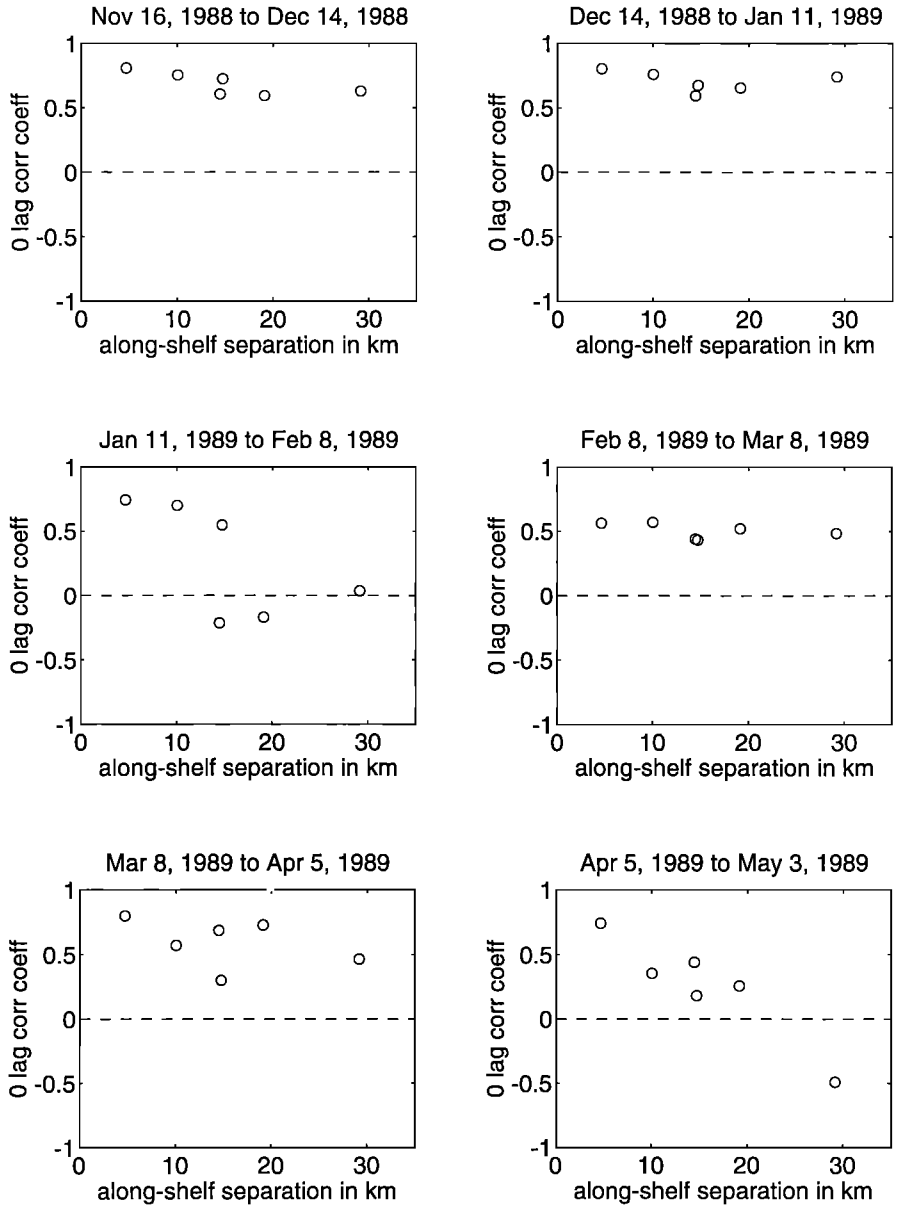

Figure 9. Correlations of near-surface cross-shelf velocity u as a function of along-shelf mooring separation for six 1-month periods between November 1988 and May 1989. Correlations with wind stress are also presented in Table 5.

Table 5. Correlations of Near-Surface u With Along-Shelf Wind Stress Over 1-Month Periods

	Period					
	Nov. 16, 1988, to Dec. 14, 1988	Dec. 14, 1988, to Jan. 11, 1989	Jan. 11, 1989, to Feb. 8, 1989	Feb. 8, 1989, to March 8, 1989	March 8, 1989, to April 5, 1989	April 5, 1989, to May 3, 1989
Wind σ, dyn cm^{-2}	0.74	0.72	0.65	1.02	0.95	0.71
u scale, km	30	30	15	30	30	15
Mooring						
G3	0.77	0.82	0.44	0.61	0.81	0.56
C3	0.78	0.63	0.41	0.60	0.63	0.76*
NCCCS C3	0.68	0.67	0.38	0.79	0.79	0.70
M3	0.71	0.73	0.69	0.75	0.73	0.18

Rough estimates of u correlation scales and the standard deviations, σ, of τ^y for each month are also shown.
*Short record.

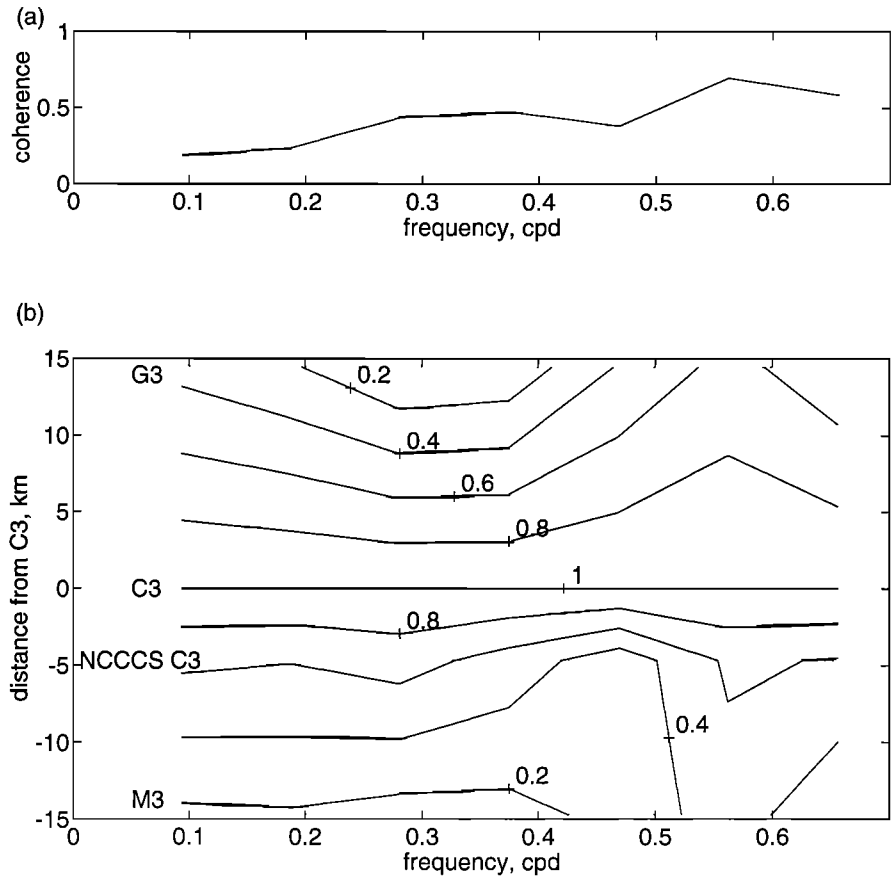

Figure 10. (a) Coherence of near-surface u at C3 with τ^y. Coherence of other near-surface u records with τ^y also decline with decreasing frequency. (b) Coherence of near-surface u with distance from C3. The 90% confidence level is 0.45, and the 95% confidence level is 0.50.

correlation scales (and correlations with along-shelf wind stress) which are most evident from late January to mid-February and increase again in late February.

During April, correlation scales are reduced probably by the presence of a mesoscale feature over much of the shelf. This feature, described by *Largier et al.* [1993], originates from offshore as indicated by its high temperature and low salinity [*Alessi et al.*, 1991]. It is responsible for strong equatorward flow over the study area despite the absence of persistent equatorward wind forcing (Figure 8), and it affects both the near-surface circulation and the heat and salt balances [*Dever and Lentz*, 1994]. Similar features have also been observed at different times in previous years [*Lentz*, 1987; *Washburn et al.*, 1993].

Largier et al. [1993] postulate that oceanic mesoscale features commonly occur over the northern California shelf and that they are a significant source of forcing for shelf circulation at periods longer than 10 days for which wind stress variance is low. During the winter 1988–1989, along-shelf wind stress variance peaks at periods between 2.5 and 5 days [*Dever*, 1995]. If wind stress forcing dominates at short periods and oceanic mesoscale variability is the primary source of forcing for longer periods, then spatial coherence of near-surface u should be highest in the wind band as there is no reason to expect oceanic mesoscale forcing to be two-dimensional. Figure 10 lends some support to this idea. Both coherence with the wind stress and along-shelf coherence are largest at the same frequencies and decline for longer periods where oceanic mesoscale forcing may become more important.

The association of the longest spatial scales of near-surface u with wind stress forcing is also supported by empirical orthogonal functions (EOFs) of near-surface u during SMILE and NCCCS (Figures 11 and 12). The lowest mode, which accounts for 57% of the variance, is highly correlated (0.76) with along-shelf wind stress, is important throughout the November to May period, and exhibits little along-shelf structure. Higher modes have more complex spatial structures and are uncorrelated with the wind stress. They become important on timescales of weeks when correlation scales are reduced. Modes 2 and 3 become important during January and early February. Together they represent u fluctuations at G3 (in January) and C3 and NCCCS C3 (in February). Mode 2 again becomes important in late April when it represents offshore flow at M3 and onshore flow at G3. The timescales of the higher modes, their intermittent nature, and the lack of correlation with wind stress all suggest that they are not associated with wind forcing.

4.2. Monthly Variation in Cross-Shelf Velocity Correlation Between SMILE C3 and NCCCS C3

Velocity measurement at most SMILE and NCCCS moorings was limited to the near surface (10 m). However, C3 was instrumented throughout the water column. The C3 sites of

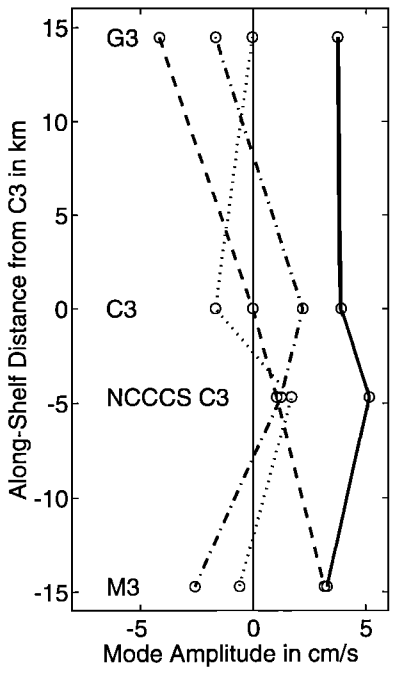

Figure 11. Along-shelf structure of near-surface u empirical orthogonal functions (EOFs). The solid line indicates mode 1 which accounts for 57% of the total variance. Modes 2, 3, and 4, indicated by the dashed, dash-dotted, and dotted lines, account for 24%, 13%, and 5% of the total variance, respectively.

NCCCS, SMILE, and STRESS were located approximately 4 km apart in the along-shelf direction. They provide an opportunity to examine correlation in the along-shelf direction for near-surface, middepth, and near-bottom depths. Correlations between these two sites (Figure 13) showed that near-surface correlations were the highest and that monthly trends in correlations were the same at all depths. This indicates that remarks concerning correlation scales of near-surface u may also be applicable to interior and near-bottom u.

5. Discussion

On wind-forced shelves, CTWs and Ekman theory have been compared quantitatively with observed interior [e.g., *Chapman*, 1987] and boundary layer flows [e.g., *Dever*, 1995; *Lentz*, 1992]. CTWs and Ekman theory both imply correlation scales for u and v. For v, velocities associated with CTWs are much larger than surface and bottom Ekman velocities so that the wind-forced v is dominated by the CTW response throughout the water column. *Brink et al.* [1987, 1994] have examined the scales of motion implied by full (i.e., no long-wave assumption) CTWs and found that v is resonant for low wavenumber along-shelf wind stress variability implying correlation scales of 100–200 km.

Brink et al. [1987, 1994] also found u velocities associated with CTWs to be more sensitive to high wavenumber along-shelf wind stress with scales of 15 km or less, implying similarly short correlation scales for u forced by CTWs. However, unlike v the character of the total wind-forced u is not determined mainly by the CTW response. Cross-shelf boundary layer transports are the same magnitude as CTW cross-shelf transports, and because they are confined to relatively thin layers, the velocities associated with them are greater [*Dever*, 1995]. Therefore, in the absence of other processes, theoretical u correlation scales within the surface and bottom boundary layers should reflect those of along-shelf wind stress and interior v, respectively. Over the northern California shelf these along-shelf correlation scales are 100 km or more (Figure 3) and over 60 km (Figure 4).

The theoretical correlation scales above are larger than those observed on the northern California shelf. This is especially true for u. Observed v correlation scales are next discussed, and a more extensive discussion of u correlation scales follows.

Correlations of v estimated in this study and previously [*Winant et al.*, 1987] over the northern California shelf and elsewhere [*Kundu and Allen*, 1976] are in many ways consistent with those expected from CTWs. The correlation scale of v estimated here, though almost certainly less than the limits implied by CTWs, is greater than 60 km (Figure 4). Maximum lagged v along-shelf correlation coefficients tend to exhibit behavior consistent with CTWs in that southern velocity records generally lead northern velocity records by about 3 to 12 hours (Table 3). Application of CTWs is limited to the midshelf and outer shelf where surface and bottom boundary layers can be considered thin. The increasing importance of mesoscale processes offshore and the cross-shelf structure of CTW modes on the northern California shelf [*Chapman*, 1987] would suggest that along-shelf correlation scales decrease offshore. In this study, examination of along-shelf correlation scales of v was limited to CODE-2 observations between 60 and 130 m. Within this region, little cross-shelf variation in along-shelf v correlations is evident except for near-surface observations where along-shelf v correlations at the 130 m isobath are reduced slightly relative to those at the 60 and 90 m isobaths. This is a possible indication that mesoscale processes are more important near the surface.

In the cross-shelf direction, v is generally correlated from 60 to 130 m. Despite its smaller magnitude and possible effects of local bathymetry, inner-shelf v (30 m) is also significantly correlated out to the midshelf (90 m), arguing for a similar response in v to wind forcing over much of the shelf. Maximum lagged v cross-shelf correlations tend to exhibit behavior consistent with two-dimensional upwelling models in that inshore velocity records generally lead offshore velocity records (Table 4), suggesting a more rapid response to wind forcing in shallow water.

Along-shelf correlation scales of u are much shorter than those of v and were best resolved by near-surface measurements during SMILE and NCCCS (Figure 5). Near-surface and near-bottom along-shelf scales of u are substantially less than those of along-shelf wind stress and interior along-shelf velocity which set the scales of u in models of surface and bottom boundary layers. Figures 8, 9, 10, and 12 and Table 5 all suggest that wind forcing is associated with the longest scales of near-surface u in winter and spring and that other processes act to reduce correlation scales on periods of several weeks to 1 month (Figures 8 and 9 and Table 5). The timescales and spatial structures of variability in short-scale u are consistent with those of mesoscale features. The similar time variation of correlations between two nearby moorings at near-surface, middepth, and near-bottom locations (Figure 13) suggests the processes which act to reduce near-surface u correlation are also important throughout the water column.

Examination of u along-shelf correlation scales was limited to the period between November 1988 and May 1989. This

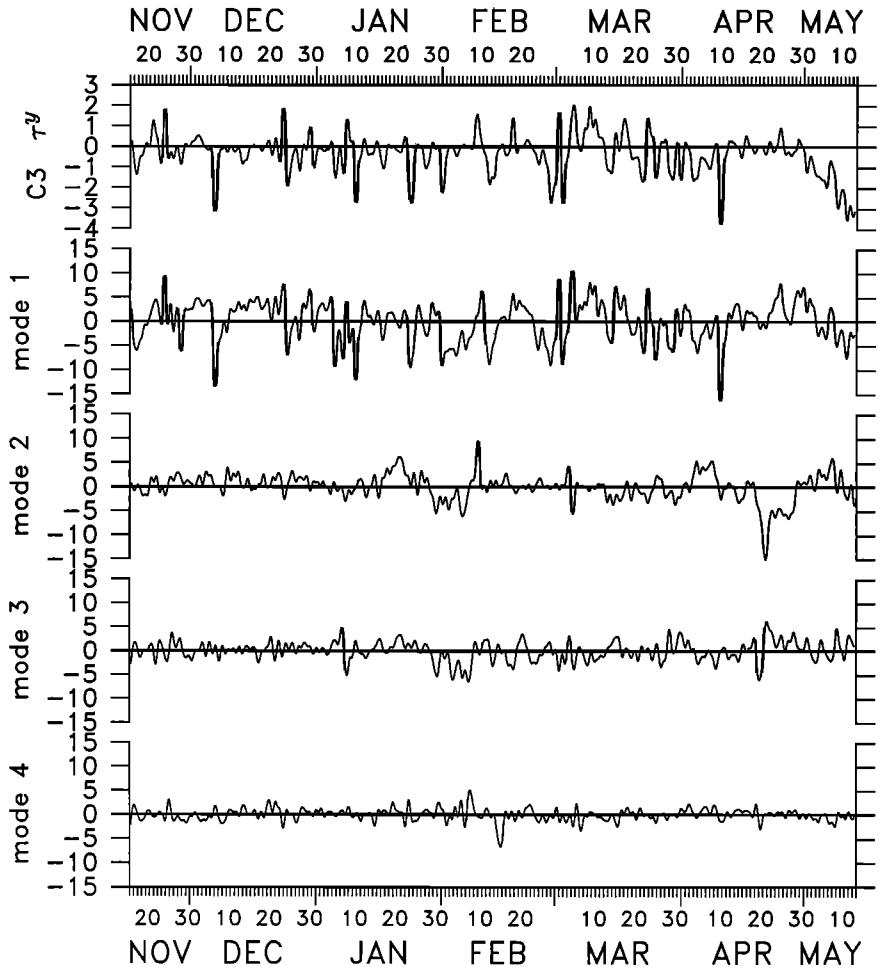

Figure 12. Time series of τ^y (dyn cm^{-2}) and near-surface u (cm s^{-1}) EOF modes. To lengthen the EOF time series into late April, the SMILE time series at C3 has been extended by patching the 8.5 and 11.5 m time series together. The correlation coefficient of mode 1 with τ^y at C3 is 0.76. Higher modes are uncorrelated with τ^y.

period covered the winter and spring storm season and ended days after the spring transition to upwelling; hence the applicability of the above observations to u correlation scales in the summer (upwelling) season is uncertain. Section 4.1 showed that for some periods of 1 month or more, along-shelf correlation scales were at least 30 km, the maximum along-shelf mooring separation in SMILE. Though 30 km is the minimum along-shelf mooring separation during CODE-2, making it difficult to compare spatial scales, a similar treatment of summer CODE-2 data revealed no time when correlation scales were as great as 30 km. This suggests the possibility of seasonal (or interannual) variation in along-shelf scales of near-surface u. Seasonal variability could be due to greater offshore mesoscale activity in the summer [*Kosro et al.*, 1991] which would tend to shorten correlation length scales in summer. Offshore mesoscale variability in summer may or may not be related to instability of an upwelling front. *Barth* [1994] examined the development of frontal instabilities and found that the timescale for development of a short-wavelength (20 km) baroclinic instability was about 1.5 days. In winter, wind forcing events tend to be relatively brief and do not lead to the development of an upwelling front. After the spring transition to upwelling, a front develops and moves offshore. Instabilities associated with this front, and with later fronts caused by wind stress relaxation and subsequent upwelling, are a ready source of three-dimensional variability in summer. In this way, upwelling favorable winds which persist long enough to cause the development of an upwelling front may be an indirect source of short correlation length scales.

The importance of short-scale wind stress in reducing correlation scales of interior u remains uncertain. Though along-shelf wind stress is highly correlated over distances of up to 130 km for both SMILE and CODE-2 (Figure 3), aircraft observations make it clear that short-scale wind stress is present south of Point Arena [*Winant et al.*, 1988; *Dorman et al.*, 1995]. Neither the aircraft observations nor the available buoy observations allow the estimation of the complete wavenumber spectrum. Though inclusion of an estimated short-scale (down to 10 km) wind stress in a stochastic model [*Brink et al.*, 1994] reduces interior u scales, observed u fluctuations are more energetic than predictions of the linear model.

Cross-shelf correlation scales of u are about 10 km. These correlation scales extend over a substantial portion of the northern California shelf and are only about 5 km less than the cross-shelf correlation scales of v. There is some indication that u is more weakly correlated from the inner shelf to the

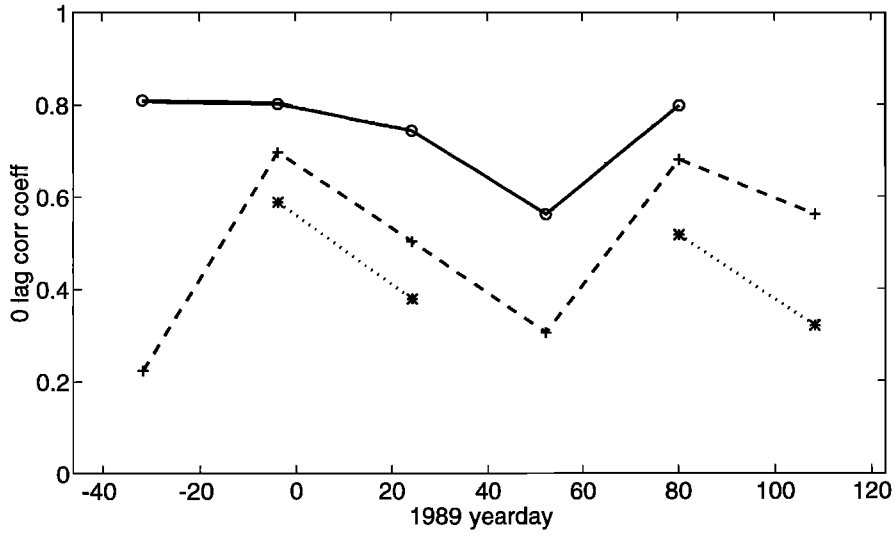

Figure 13. Correlations of cross-shelf velocity u between SMILE and NCCCS C3 moorings. Near-surface (solid), middepth (dashed), and near-bottom (dotted) instruments are considered for six one-month periods between November 1988 and May 1989. Though correlations are highest between near-surface instruments, monthly trends are similar for all instrument depths.

midshelf (60 to 90 m, a distance of approximately 5 km) than from the midshelf to the outer shelf (90 to 130 m, a distance of ~8 km). Because we expect offshore mesoscale features to reduce correlation scales over the outer shelf rather than the inner shelf, it is likely some other process is responsible for this. As most of the observations used in Table 4 come from summer, one reasonable explanation is near-shore variability caused by relaxation from upwelling [*Send et al.*, 1987]. During relaxation events, northward advection of warm saline water from Point Reyes occurs in a wedge confined primarily to the inner-shelf and midshelf locations. This could cause a break in the character of the flow field between the 60 and 90 m isobaths. This type of three-dimensional variability could overwhelm the wind-driven signal especially over the inner shelf where models suggest wind-driven u is reduced relative to deeper water by the overlap of surface and bottom stresses [*Mitchum and Clarke*, 1986; *Lentz*, 1994].

6. Summary

Correlations of subtidal cross-shelf (u) and along-shelf (v) velocities are estimated as a function of along-shelf and cross-shelf distance using moored time series from several field programs over the northern California shelf. Distances over which velocities are significantly correlated are termed correlation scales.

Over periods of 4–6 months, correlation scales of v are resolved in both the along-shelf and cross-shelf directions. In the along-shelf direction, v is significantly correlated for distances greater than 60 km, the maximum mooring separation. In the cross-shelf direction, v is generally correlated between the 60 and 130 m isobaths (10–15 km). Correlations of v show little dependence on instrument depth; subsurface v is perhaps more highly correlated than surface v.

Correlation scales of u over periods of 4–6 months are much smaller than those of v and are often not resolved by minimum mooring separations. Moorings deployed in SMILE and NCCCS do resolve along-shelf correlation scales of near-surface u and indicate that they are 15–20 km. Along-shelf correlation scales of subsurface u are not well resolved by available data but are less than 25 km. In the cross-shelf direction, u correlation scales are ~10 km. There is some indication that u is more highly correlated between the 90 and 130 m isobaths than between the 60 and 90 m isobaths.

To investigate further the processes which determine along-shelf correlation scales of u, SMILE and NCCCS records from November 1988 to May 1989 were examined in greater detail. Monthly variation of correlation scales was compared to correlation with along-shelf wind stress, the heat balance, and other descriptive information about shelf circulation. During several months the along-shelf correlation scale of near-surface u was at least 30 km, the maximum mooring separation, and it was always greater than 4 km, the minimum mooring separation. Along-shelf correlation scales were generally long when correlation of velocity with wind stress was high and short when correlation with wind stress was low. Short correlation scales coincided with three-dimensional heat, salt, and volume balances. During April 1989, short correlation scales coincided with the intrusion of an offshore mesoscale feature onto the shelf. Along-shelf correlations of near-surface, middepth, and near-bottom u between two nearby (4 km) sites showed near-surface correlations were highest but that monthly trends in correlations were similar at all depths.

Acknowledgments. This work was done as part of my thesis in the MIT/WHOI Joint Program in Oceanography. Financial support was provided by NSF grant OCE 91–15713. I thank especially my advisor S. Lentz and also committee members J. Price, K. Brink, R. Beardsley, P. Malanotte-Rizzoli, and R. Weller for helpful discussions and comments. The careful comments of two reviewers are also appreciated. Special thanks are also extended to B. Butman at USGS Woods Hole and J. Trowbridge (WHOI) for making available STRESS data and to J. L. Largier (SIO, University of Cape Town, South Africa), B. A. Magnell (EG&G), and C. D. Winant (SIO), who generously made available NCCCS data. Support for preparation of the manuscript at SIO was provided by The Mellon Foundation and by the Minerals Management Service under cooperative agreement 14-35-0001-30571. Woods Hole Oceanographic Institution contribution 9187.

References

Alessi, C. A., S. J. Lentz, and R. C. Beardsley, The shelf mixed layer experiment (SMILE): Program overview and moored and coastal array data report, *WHOI Tech. Rep. 91-39*, 211 pp., Woods Hole Oceanogr. Inst., Woods Hole, Mass., 1991.

Allen, J. S., Models of wind-driven currents on the continental shelf, *Annu. Rev. Fluid Mech.*, *12*, 389–433, 1980.

Allen, J. S., et al., Physical oceanography of continental shelves, *Rev. Geophys.*, *21*, 1149–1181, 1983.

Barth, J. A., Short-wavelength instabilities on coastal jets and fronts, *J. Geophys. Res.*, *99*, 16,095–16,115, 1994.

Beardsley, R. C., and S. J. Lentz, The Coastal Ocean Dynamics Experiment collection: An introduction, *J. Geophys. Res.*, *92*, 1455–1464, 1987.

Beardsley, R. C., C. E. Dorman, C. A. Friehe, L. K. Rosenfeld, and C. D. Winant, Local atmospheric forcing during the Coastal Ocean Dynamics Experiment, 1, A description of the marine boundary layer and atmospheric conditions over a northern California upwelling region, *J. Geophys. Res.*, *92*, 1467–1488, 1987.

Brink, K. H., The near-surface dynamics of coastal upwelling, *Prog. Oceanogr.*, *12*, 223–257, 1983.

Brink, K. H., Coastal-trapped waves and wind-driven currents over the continental shelf, *Annu. Rev. Fluid Mech.*, *23*, 389–412, 1991.

Brink, K. H., D. C. Chapman, and G. R. Halliwell, A stochastic model for wind-driven currents over the continental shelf, *J. Geophys. Res.*, *92*, 1783–1797, 1987.

Brink, K. H., J. H. LaCasce, and J. D. Irish, The effect of short-scale wind variations on shelf currents, *J. Geophys. Res.*, *99*, 3305–3314, 1994.

Chapman, D. C., Application of wind-forced, long, coastal-trapped wave theory along the California coast, *J. Geophys. Res.*, *92*, 1798–1816, 1987.

Csanady, G. T., *Circulation in the Coastal Ocean*, 279 pp., D. Reidel, Norwell, Mass., 1982.

Dever, E. P., Subtidal cross-shelf circulation on the northern California shelf, Ph.D. thesis, Mass. Inst. of Technol./Woods Hole Oceanogr. Inst., Woods Hole, 1995.

Dever, E. P., and S. J. Lentz, Heat and salt balances over the northern California shelf in winter and spring, *J. Geophys Res.*, *99*, 16,001–16,017, 1994.

Dorman, C. E., A. G Enriquez, and C. A. Friehe, Structure of the lower atmosphere over the northern California coast during winter, *Mon. Weather Rev.*, *123*, 2384–2404, 1995.

EG&G, Inc., Northern California Coastal Circulation Study data report no. 2: Main measurement program, March–August 1988, *Oceanogr. Serv. Rep. NCCCS-89-17*, 2 vols., 442 pp., Washington Anal. Serv. Cent., Waltham, Mass., Sept. 1989.

EG&G, Inc., Northern California Coastal Circulation Study data report no. 3: Main measurement program, August 1988–March 1989, *Oceanogr. Serv Rep. NCCCS-90-4*, 2 vols., 344 pp., Washington Anal. Serv. Cent., Waltham, Mass., March 1990a.

EG&G, Inc., Northern California Coastal Circulation Study data report no. 4: Main measurement program, March–October 1989, *Oceanogr. Serv. Rep. NCCCS-90-5*, 2 vols., 326 pp., Washington Anal. Serv. Cent., Waltham, Mass., Aug. 1990b.

Fredericks, J. J., J. H. Trowbridge, A. J. Williams III, S. J. Lentz, B. Butman, and T. F. Gross, Fluid mechanical measurements within the bottom boundary layer over the northern California continental shelf during STRESS, *WHOI Tech. Rep. 93-32*, 116 pp., Woods Hole Oceanogr. Inst., Woods Hole, Mass., 1993.

Halliwell, G. R., Jr., and J. S. Allen, The large-scale coastal wind field along the west coast of North America, 1981–1982, *J. Geophys. Res.*, *92*, 1861–1884, 1987.

Janowitz, G. S., and L. J. Pietrafesa, A model and observations of time-dependent upwelling over the mid-shelf and slope, *J. Phys. Oceanogr.*, *10*, 1574–1583, 1980.

Kosro, P. M., et al., The structure of the transition zone between coastal waters and the open ocean off northern California, winter and spring 1987, *J. Geophys. Res.*, *96*, 14,707–14,730, 1991.

Kundu, P. K., and J. S. Allen, Some three-dimensional characteristics of low-frequency current fluctuations near the Oregon coast, *J. Phys. Oceanogr.*, *6*, 181–199, 1976.

Largier, J. L., B. A. Magnell, and C. D. Winant, Subtidal circulation over the northern California shelf, *J. Geophys. Res.*, *98*, 18,147–18,179, 1993.

Lentz, S. J., A heat budget for the northern California shelf during CODE 2, *J. Geophys. Res.*, *92*, 14,491–14,509, 1987.

Lentz, S. J., The surface boundary layer in coastal upwelling regions, *J. Phys. Oceanogr.*, *22*, 1517–1539, 1992.

Lentz, S. J., Current dynamics over the northern California inner shelf, *J. Phys. Oceanogr.*, *25*, 2461–2478, 1994.

Lentz, S. J., U.S. contributions to the physical oceanography of continental shelves in the early 1990s, *Rev. Geophys.*, *33*, 1225–1236, 1995.

Lentz, S. J., and D. C. Chapman, Seasonal differences in the current and temperature variability over the northern California shelf during the Coastal Ocean Dynamics Experiment, *J. Geophys. Res.*, *94*, 12,571–12,592, 1989.

Lentz, S. J., and J. H. Trowbridge, The bottom boundary layer over the northern California shelf, *J. Phys. Oceanogr.*, *21*, 1186–1201, 1991.

Limeburner, R. (Ed.), CODE-2: Moored array and large-scale data report, *WHOI Tech. Rep. 85-35*, 234 pp., Woods Hole Oceanogr. Inst., Woods Hole, Mass., 1985.

Mitchum, G. T., and A. J. Clarke, The frictional nearshore response to forcing by synoptic scale winds, *J. Phys. Oceanogr.*, *16*, 934–946, 1986.

Rosenfeld, L. (Ed.), CODE-1: Moored array and large-scale data report, *WHOI Tech. Rep. 83-23*, 186 pp., Woods Hole Oceanogr. Inst., Woods Hole, Mass., 1983.

Send, U., R. C. Beardsley, and C. D. Winant, Relaxation from upwelling in the Coastal Ocean Dynamics Experiment, *J. Geophys. Res.*, *92*, 1683–1698, 1987.

Smith, R. L., A comparison of the structure and variability of the flow field in three coastal upwelling regions: Oregon, northwest Africa, and Peru, in *Coastal Upwelling, Coastal Estuarine Sci.*, vol. 1, edited by F. A. Richards, pp. 107–118, AGU, Washington, D. C., 1981.

Smith, R. L., The physical processes of coastal ocean upwelling systems, in *Upwelling in the Ocean: Modern Processes and Ancient Records*, edited by C. P. Summerhayes et al., pp. 39–64, John Wiley, New York, 1995.

Strub, P. T., J. S. Allen, A. Huyer, R. L. Smith, and R. C. Beardsley, Seasonal cycles of currents, temperatures, winds, and sea level over the northeast Pacific continental shelf: 35°N to 48°N, *J Geophys. Res.*, *92*, 1507–1526, 1987.

Trowbridge, J. H., and S. J. Lentz, Asymmetric behavior of an oceanic bottom boundary layer above a sloping bottom, *J. Phys. Oceanogr.*, *21*, 1171–1185, 1991.

Washburn, L., M. S. Swenson, J. L. Largier, P. M. Kosro, and S. R. Ramp, Cross-shelf sediment transport by an anticyclonic eddy off northern California, *Science*, *261*, 1560–1564, 1993.

Winant, C. D., Longshore coherence of currents on the southern California shelf during the summer, *J. Phys. Oceanogr.*, *13*, 54–64, 1983.

Winant, C. D., R. C. Beardsley, and R. E. Davis, Moored wind, temperature, and current observations made during Coastal Ocean Dynamics Experiments 1 and 2 over the northern California shelf and upper slope, *J. Geophys. Res.*, *92*, 1569–1604, 1987.

Winant, C. D., C. E. Dorman, C. A. Friehe, and R. C. Beardsley, The marine layer off northern California: An example of supercritical channel flow, *J. Atmos. Sci.*, *45*, 3588–3605, 1988.

E. P. Dever, Center for Coastal Studies 0209, Scripps Institution of Oceanography, University of California, San Diego, 9500 Gilman Drive, La Jolla, CA 92093-0209. (e-mail: dever@coast.ucsd.edu)

(Received April 10, 1996; revised September 19, 1996; accepted October 3, 1996.)